Journal of Engineering Research and Reports

19(2): 20-25, 2020; Article no.JERR.62557
ISSN: 2582-2926

Design of Solar Blind Photodetectors for Communication with Green Signal (λ= 0.532μm) in Space. Part II

Samson Mil'shtein[1*] and Dhawal Asthana[1]

[1]Advanced Electronic Technology Center, ECE Dept., UMass, Lowell, MA 01854, USA.

Authors' contributions

This work was carried out in collaboration between both authors. The main idea and conceptual structure of the photodetector were offered by author SMS. The integrated power supply (solar cell) is the idea of the author DA who finalized the modeling on commercial software. Both authors read and approved the final manuscript.

Article Information

DOI: 10.9734/JERR/2020/v19i217227
Editor(s):
(1) Dr. Pierre-Olivier Logerais, Université Paris-Est Créteil, France.
Reviewers:
(1) Rashid Ali Fayadh, Middle Technical University, Iraq.
(2) Mohammed Saad Talib, University of Babylon, Iraq.
Complete Peer review History: http://www.sdiarticle4.com/review-history/62557

Original Research Article

Received 04 September 2020
Accepted 09 November 2020
Published 02 December 2020

ABSTRACT

The areas of Free Space Optical (FSO) communication and high-speed Visible Light Communication (VLC) offer potential for very high-speed data transmission. Favorable attributes including high frequency and wider bandwidths that can enable transmission speeds of the order 100Gb/s, associated with the visible region of the electromagnetic spectrum make it preferable for allowing communication among satellites and ground stations, under-water communication, etc. However, limitations associated with spectral absorption characteristics of the propagating media have stymied further development of such technologies.

Aims: Commercial lasers operating in red, green and blue lights combined with three photodetectors, each sensitive to selected wavelengths (colors) present basics of long-distance optical communication system. The current study (Part II) depicts the design and operation of a solar-blind photodetector capable to work explicitly with green wavelength of 532nm.

Study Design and Results: The structure of the solar-blind photodetector consists of two sections made of $In_xGa_{1-x}N$ (Indium Gallium Nitride) heterostructure, (where x denotes the mole fraction)-a filter and a double barrier tunneling diode. The topmost approximately 1μm thick section acts as a

**Corresponding author: Email: Samson_Mil'shtein@uml.edu;*

filter and as a p-i-n solar cell providing the required voltage bias to the photodiode. The filter with Eg (Energy Band Gap)=2.33eV absorbs all photons having wavelengths shorter than 532nm. The double barrier tunneling photodiode which comprises the lower section operates with Eg=2.28eV. It consists of an n-type lightly doped quantum well having a width of 2.5nm housed between two lightly doped barriers of 10nm thickness. The 0.12μm topmost and bottom regions of the photodiode are doped with p and n ($2\times10^5 cm^{-3}$) type impurities, respectively. The illuminated cross-section area of the device is finalized at $1mm^2$.

Keywords: Optical; detectors; wireless communication; solar-blind photodetector.

1. INTRODUCTION

Free space optical communication and wireless optical communication are expected to have the possibility to use stand-alone red, green or blue signal systems [1-2]. Promising results for responsivity and frequency response recorded for polymer-based photodetectors in the context of (VLC), discussed in [3], intensify the scope for further research and development in this field. In the first part of our study [1], which addressed the design of a solar-blind photodetector sensitive to the red signal, we described the status of the development of solar-blind photodetectors. Reviewing the state-of-the-art of solar blind photodetector technologies [4-7], we discovered that the claim of many novel designs of "solar blindness" is not very accurate [8-11]. While operation in the non-visible (particularly middle and far-UV) regions may obviate solar blindness as discussed in [12-13], the definition of solar blindness must imply non-responsiveness to solar radiation under all circumstances of operation. Also, the completely solar-blind detector should have a discrimination window offering a demarcated band of accepted wavelengths, instead of a single value of threshold wavelength determining the spectral response.

Since most of the FSO and VLC communication technologies make use of commercial lasers that operate at discrete wavelengths with intensities comparable to that of the ambient solar irradiance, sensors which are not receptive to a very small band of laser radiation end up being very noisy in operation. In order to eliminate this hurdle, we present the design of our photodetector which is sensitive to a very small band of frequency within the green band of visible light. Most of the solid state-based commercial lasers for green light emit at wave lengths neighboring 532nm. To match such signals, we have realized the solar-blind photodetector which is sensitive within the range of wavelengths given by (532nm-543nm) using $In_xGa_{1-x}N$ heterostructures [14-15].

2. MODELLING OF THE DEVICE

As shown in Fig. 1, the structure consists of two sections: a filter and a double barrier tunneling diode. The 0.8μm thick topmost section which is exposed to external illumination, forms a p-i-n solar cell made up of $Ga_{0.72}In_{0.28}N$ with Eg=2.33eV. It acts as a filter to absorb all photons with wavelengths shorter than 532nm and also acts as a solar cell providing the reverse bias to the photodetector. The filter structure consists of a 0.5μm thick intrinsic layer sandwiched between equally doped 0.1μm thick p- and n-type terminals ($N_a=N_d=10^{18}cm^{-3}$).

The photodetector which comprises the lower section operates on the basis of double barrier tunneling phenomenon [3]. It consists of a 2.5nm thick n-type doped quantum well made of $In_xGa_{1-x}N$ (x=0.32) with E_g=2.28eV, housed between two 10nm thick (each) n-type doped barriers made of $In_xGa_{1-x}N$ (x=0.18).The 0.12μm thick top and bottom electrodes in the photodiode, made of $In_xGa_{1-x}N$ (x=0.32) are p- and n-type doped respectively ($N_a=N_d=1.2\times10^5 cm^{-3}$). The objective of limiting the number of discrete energy levels in the finite potential well (quantum well) has dictated the value of its thickness and the choice of the barrier height which is realized as E_g=2.76eV as shown in Fig. 2.

The connection between the negative terminal of the solar cell and the p-type doped electrode of the photodetector is realized by an aluminum contact extending along the rim of the device. A 0.1μm thick intrinsic layer of $Ga_{0.72}In_{0.28}N$, shown in Fig. 1, acts as a non-opaque insulating layer between these terminals."Solar blindness" of the structure can be ensured by drawing an analogy from the analysis conducted in Part I [2]. With the intensity of a narrow band of green present in the solar spectrum being considerably less than that

of a laser, the signal in the photodetector due to the former will be negligible compared to that from the laser.

3. RESULTS AND DISCUSSION

Two separate analyses were conducted on SILVACO to evaluate the performances of the photodetector and the solar cell. The output current density of the reverse-biased photodetector, when irradiated with a 543nm laser beam having intensity=1W/cm^2,is displayed in Fig. 3 for values of different reverse bias voltages at the p-type electrode depicted along the x-axis.

The performance characteristics of the solar cell depicted in Fig. 4, have been obtained through simulations with the solar spectrum. The open-circuit voltage (V_{oc}) was obtained at 1.8V, the comparatively high value of which can be attributed to the high energy band gap value of $Ga_{0.72}In_{0.28}N$.

The joint operation of the solar cell and the photodetector is indicated in Fig. 5, where the solar cell generates photocurrent to create a potential drop across the load resistor (very low value) and reverse bias for the photodetector with an approximate value of 1.8V across its terminals. The photodetector then generates current in a direction opposite to the direction of current from the solar cell.

Owing to the high intensity of the laser for the narrow band of green, larger values of current are generated by the photodetector (130mA/cm^2) which dominate the solar cell characteristics (8.5mA/cm^2) and let it operate as a diode in the forward-biased region. Operation in this region increases the voltage drop across the solar cell. Changes in direction and value of the net current preserve the reverse bias across the photodetector. As a result, the operating point for the photodetector is shifted along the curve depicted in Fig.3 accounting for minimal change in current to obviate stable operation.

Small signal AC analysis for the photodetector upon the incidence of laser light having intensity=1W/cm^2 was also conducted. As the frequency was varied from 0.1 MHz to 1000 GHz, as shown in logarithmic scale plotted along the x-axis in Fig.6., a response in the form of output current (y-axis) for a simulated specimen of the photodetector having cross-sectional area 0.5(μm)^2 (scaled down to save computational time) was recorded.

It can well be inferred from the figure that stable operation of the device is expected till cutoff-frequencies close to 100GHz.

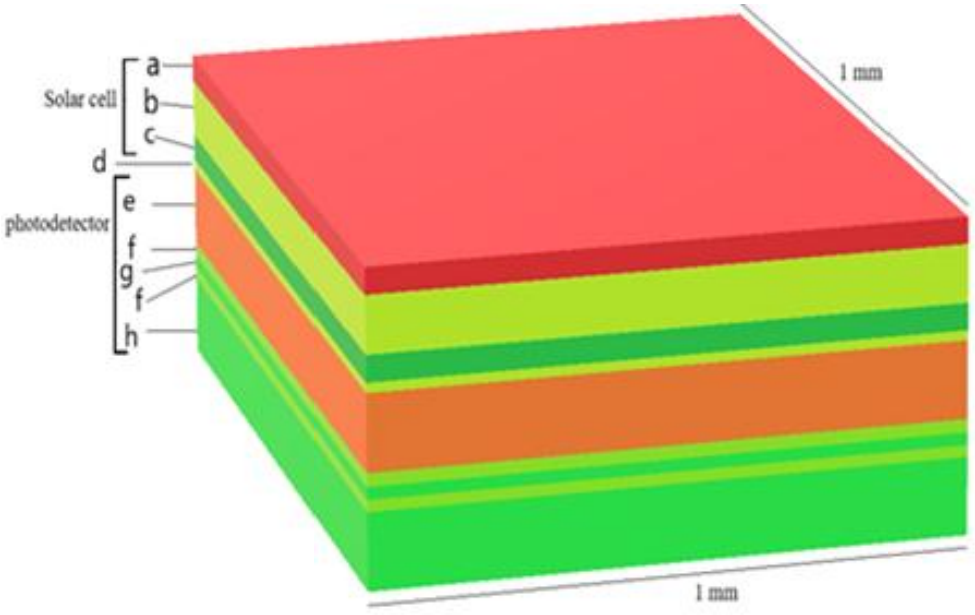

Fig. 1. a) Positive terminal of solar cell b) Intrinsic region of solar cell c) Negative terminal of solar cell d) Insulating contact e) p-type electrode of photodetector f) Lightly doped barriers g) lightly doped well h) n-type electrode of the photodetector

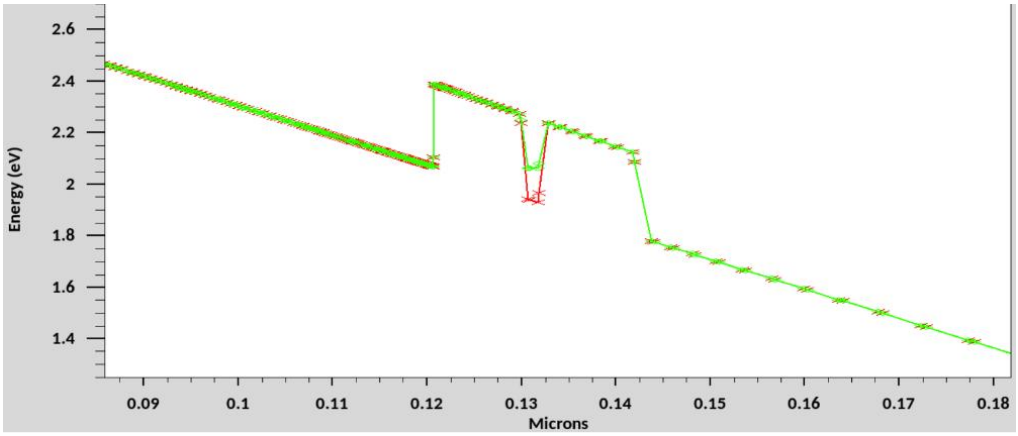

Fig. 2. Energy profile within the finite quantum well formed by $In_{0.18}Ga_{0.82}N$ barrier and $In_{0.32}Ga_{0.68}N$ (well/top/bottom) heterojunctions

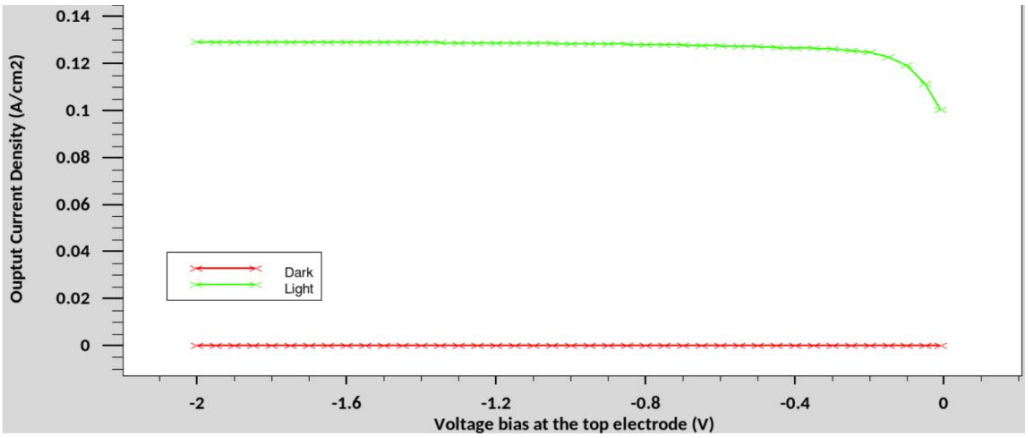

Fig. 3. Output current density in A/cm^2 obtained for irradiation with laser (shown in green) and surroundings with no irradiation (shown in red)

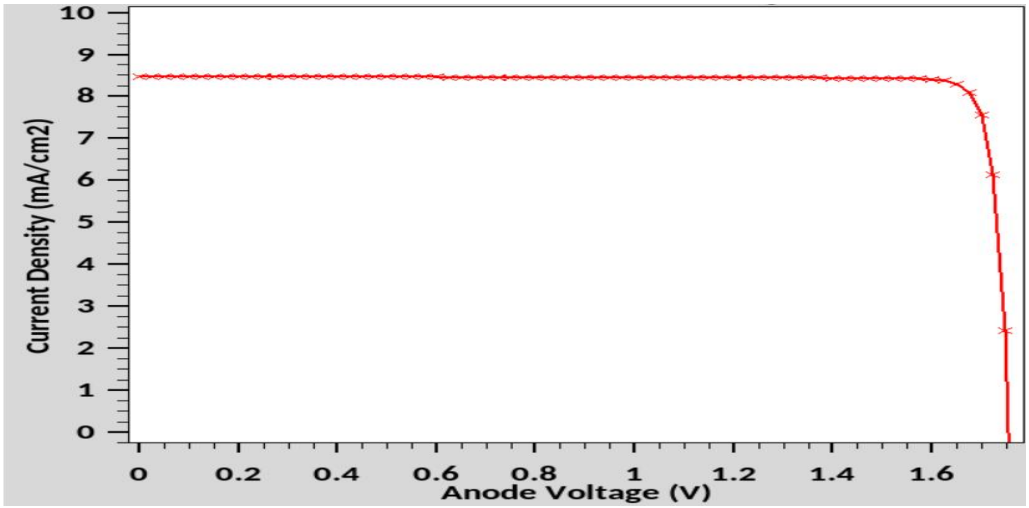

Fig. 4. Solar cell characteristics with cathode current density in mA/cm^2 plotted against anode voltage on the x-axis. (Voc obtained at current density=0)

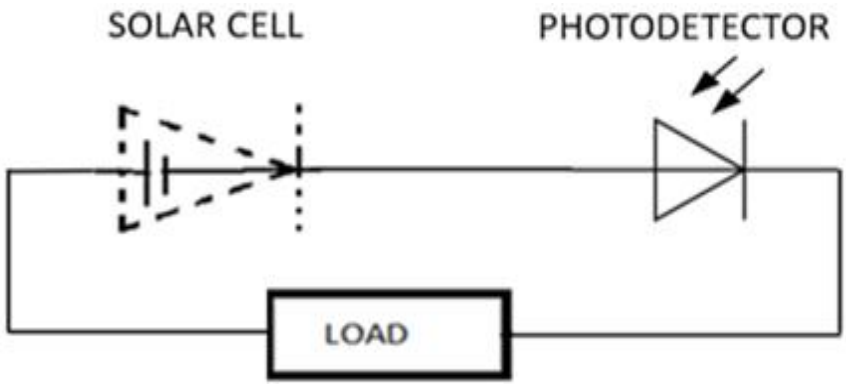

Fig. 5. Circuit diagram explaining the joint operation of the solar cell and the photodetector

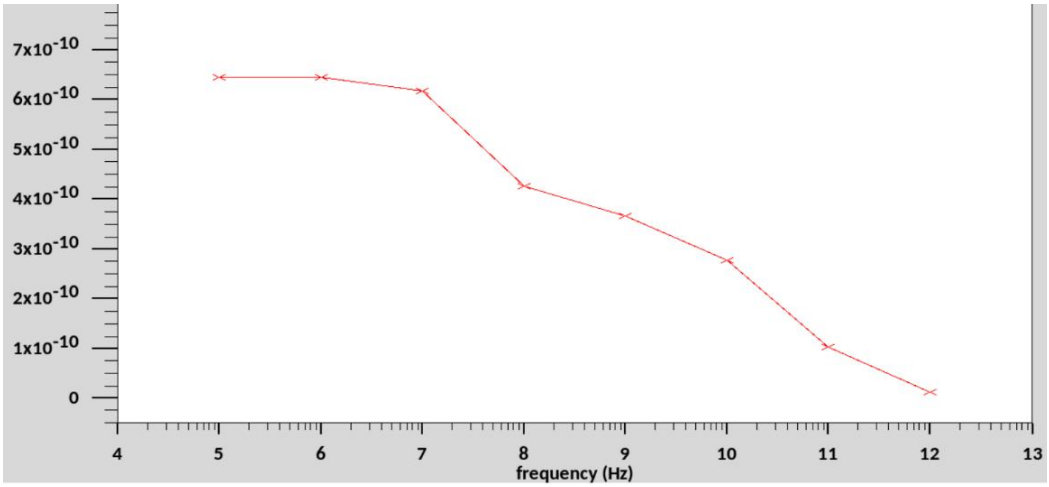

Fig. 6. Small signal AC response of the photodetector

4. CONCLUSION

The designed photodetector with sensitivity to green color wavelength λ=0.532μm is totally blind to the rest of solar spectra [1-2]. Moreover, it is not sensitive to the sun radiation of the same wavelength, as the intensity of the laser signal is greater than the radiation intensity of the sun for the selected range of wavelengths. In addition, the sun spectra randomly fluctuate as the laser periodic signal is modulated in a controlled way. The presence of these two waves can be easily separated as signal and noise. Unlike some photodetectors which only provide for upper limits of threshold or cut-off wavelengths, presented in literatures [8-11], our green light sensor operates with a discrimination window [14].

The solar blind photodetector described above, sensitive to preselected green light, is part II of the overall wireless optical communication system. At the same time, this photodetector could be used as a part of the independent optical communication hardware for civil or military applications.

ACKNOWLEDGEMENTS

The authors of the manuscript would like to thank Mr. Maksym Ushakov for his contribution in the initial stages of the work.

COMPETING INTERESTS

Authors have a pending US patent application sent in October 2020.

REFERENCES

1. Samson Mil'shtein, Dhawal Asthana, Maksym Ushakov. Design of Solar Blind

Photodetectors for Communication with Red Signal (λ= 0.65μm) in Space. Part I, 2020 MRS Fall Meeting and Exhibit. (in press)
2. Samson Mil'shtein, Dhawal Asthana, "Solar blind photodetector to operate with green signal", Patent application; 2020.
3. Arredondo B, Romero B, Pena JMS, Fernández-Pacheco A, Alonso E, Ricardo Vergaz, Cristina de Dios," Visible Light Communication System Using an Organic Bulk Heterojunction Photodetector". 2013; 13:12266-12276.
4. Paschotta R. article on 'solar-blind photodetectors' in the Encyclopedia of Laser Physics and Technology, 1st edition, Wiley-VCH; 2008.
ISBN 978-3-527-40828-3,
5. Michael E. Hoenk, John J. Hennessy, Nikzad, Jewell April Shouleh, "Sensor integrated metal dielectric filters for solar-blind silicon ultraviolet detector", US Patent. 2018;10,078,142,
6. Jinsong Huang, Yanjun Fang, "Narrow band perovskite single crystal photodetectors with tunable spectral response", US Patent No. 10622161; 2020.
7. Lei Yuan, RenxuJia, Hongpeng Zhang, Yuming Zhang, "Method for manufacturing ultraviolet photodetector based on Ga_2O_3 material", US Patent No. = 10,629,766; 2020.
8. X. Chen et al. "A self-powered solar-blind photodetector with fast response based on Au/β-Ga_2O_3 nanowires array film Schottky junction," ACS Appl. Mater. Interfaces. 2016;8:4185–4191.
9. Wang X, et al. "Optimizing the performance of a beta-Ga_2O_3 solar-blind UV photodetector by compromising between photo absorption and electric field distribution," Opt. Mater. Exp. 2018;8: 2918–2927.
10. Ranran Z, et al. "A self-powered solar-blind photodetector based on a MoS2/β-Ga_2O_3 heterojunction," J. Mater. Chem. C. 2018; 6:10982–10986.
11. Zhipeng Zhang, Holger von Wenckstern, J€orgLenzner, Michael Lorenz, and Marius Grundmann, "Visible-blind and solar-blind ultraviolet photodiodes based on $(In_xGa_{1-x})_2O_3$" Appl. Phys. Lett. 2016;108:123.
12. Caputo D, G. de Cesare, Irrera F, Palma F. "Solar-blind UV photodetectors for large area applications," in IEEE Transac. on Electron Devices. 1996;43(9):1351-1356.
13. I A Lamkin, et al. Research of the solar-blind and visible-blind photodetectors, based on the AlGaN solidsolutions J. Phys; 2014, Conf. Ser. 572 012063.
14. Levinshtein ME, Rumyantsev SL, Shur M. Properties of advanced semiconductor materials: GaN, AlN, InN, BN, SiC, SiGe. Wiley, New York; 2008.
15. Mil'shtein S, Wilson S, Pillai A. "Selective Photodetector with Resonant Tunneling", Proceed. Intern. Confer. Low Dimensional Structures & Devices, Mexico 2011;11-15.

Peer-review history:
The peer review history for this paper can be accessed here:
http://www.sdiarticle4.com/review-history/62557